1560 *Biochemistry* **2010,** *49,* 1560–1567
DOI: 10.1021/bi901948j

BIOCHEMISTRY
including biophysical chemistry & molecular biology
Current Topic

Molecular Mechanisms of System Control of NF-κB Signaling by IκBα[†]

Diego U. Ferreiro[§] and Elizabeth A. Komives*[,‡]

[‡]*Department of Chemistry and Biochemistry, University of California, 9500 Gilman Drive, La Jolla, California 92093-0378 and* [§]*Laboratorio de Expresion y Plegado de Proteinas, Universidad Nacional de Quilmes, Roque Saenz Pena 352, B1876BXD Bernal, Buenos Aires, Argentina*

Received November 11, 2009; Revised Manuscript Received January 6, 2010

ABSTRACT: The NF-κB family of transcription factors responds to inflammatory cytokines with rapid transcriptional activation and subsequent signal repression. Much of the system control depends on the unique characteristics of its major inhibitor, IκBα, which appears to have folding dynamics that underlie the biophysical properties of its activity. Theoretical folding studies followed by experiments have shown that a portion of the ankyrin repeat domain of IκBα folds on binding. In resting cells, IκBα is constantly being synthesized, but most of it is rapidly degraded, leaving only a very small pool of free IκBα. Nearly all of the NF-κB is bound to IκBα, resulting in near-complete inhibition of nuclear localization and transcriptional activation. Combined solution biophysical measurements and quantitative protein half-life measurements inside cells have allowed us to understand how the inhibition occurs, why IκBα can be degraded quickly in the free state but remain extremely stable in the bound state, and how signal activation and repression can be tuned by IκB folding dynamics. This review summarizes results of in vitro and in vivo experiments that converge demonstrating the effective interplay between biophysics and cell biology in understanding transcriptional control by the NF-κB signaling module.

The NF-κB[1] signaling system is a ubiquitous immediate early response network that transduces extracellular signals from a variety of receptors, integrates the information of the physiological state, and regulates patterns of gene expression. This "signaling module" (*1*) has been implicated in a variety of cellular functions such as cell growth, proliferation, apoptosis, and stress responses and is misregulated in numerous diseases (*2*, *3*). The system is named after nuclear factor κB (NF-κB) which was originally discovered as a transcription factor present in activated B-cells that strongly activates the immunoglobulin κ-chain gene expression (*4*). In vertebrates, NF-κB connotes not a single protein but a family of polypeptides that form a combinatorial number of homo- and heterodimers of p65 (RelA), RelB, c-Rel, p50, and p52 subunits (*2*). Several inhibitors of NF-κB activity have been identified and named inhibitors of κB (IκB), including isoforms IκBα, IκBβ, and IκBε, which block the nuclear localization and transcriptional activity of p65 and c-Rel-containing NF-κB dimers (*5*), and the newest member of the family, IκBδ (*6*). In resting cells, most of the estimated 100000 NF-κB dimers are bound to IκBs, keeping the NF-κB pool mainly in the cytoplasm by inhibiting its nuclear localization and association with DNA (*7*, *8*). A variety of extracellular signals, including viral antigens and lipopolysaccharides, as well as several physiological cytokines activate extracellular receptors that initiate the assembly of the IκB kinase (IKK), which in turn phosphorylates the N-terminal signal response domain of NF-κB-bound IκBα, leading to subsequent ubiquitination and degradation by the proteasome (*9*). NF-κB dimers then translocate to the nucleus, bind DNA, and regulate transcription of numerous target genes (*10*). The large number of genes that are activated by NF-κBs show widely varying transcription levels, activation kinetics, and postinduction repression. The mechanism of this diversity is only beginning to be understood (*11*, *12*). Among the strongly activated genes is the one encoding IκBα (*13*−*15*). Newly synthesized IκBα translocates to the nucleus and binds to NF-κB, and the complex is exported from the nucleus (Figure 1) (*1*, *16*). According to this model, the NF-κB transcriptional activity can be brought back to baseline by a deceptively simple negative feedback loop. However, puzzling questions arise regarding how robustness and specificity are achieved in a cellular response system that is activated by many different ligands and subsequently activates hundreds of different genes. In addition, the time dependence of the NF-κB activity is functionally relevant in that it rises and falls rapidly and may display dampened oscillations (*1*). Quantitative models of cell signaling have recently opened new approaches to our understanding of the temporal control of the NF-κB signal response (*1*). Ordinary differential equation (ODE) flux models of this system suggest that the rates at which such a simple feedback mechanism functions depend critically on the concentrations of species, in this case, NF-κB and IκBα, and the rates at which they are produced and degraded (*17*, *18*). These studies demonstrated that the synthesis and degradation rates of IκBα are critical parameters that control the signaling by the entire NF-κB signaling module. Degradation of free IκBα, which occurs in a ubiquitin-independent but proteasome-dependent fashion, is extremely rapid, so that the intracellular half-life is less than 10 min. On the other hand, NF-κB-bound IκBα is incredibly stable, with an intracellular half-life of many hours. Once bound to NF-κB, IκBα is degraded only if it is first phosphorylated, then ubiquitinated, and finally degraded by the proteasome in a ubiquitin-dependent fashion. What are the biochemical and

[†]This work was funded by NIH P01GM071862.

*To whom correspondence should be addressed: Department of Chemistry and Biochemistry, University of California, 9500 Gilman Dr., La Jolla, CA 92093-0378. Phone: (858) 534-3058. Fax: (858) 534-6174. E-mail: ekomives@ucsd.edu.

[1]Abbreviations: IκB, inhibitor of κB proteins; NF-κB, nuclear factor κB; AR, ankyrin repeat; ARD, ankyrin repeat domain.

 Published on Web 01/07/2010

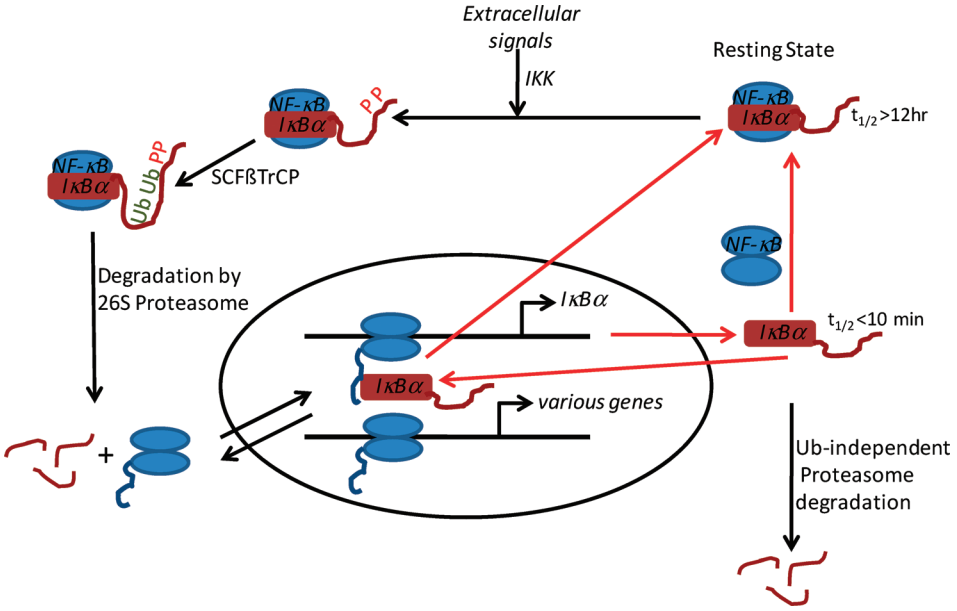

FIGURE 1: Schematic diagram of the NF-κB signaling pathway. This figure places emphasis on the role of IκBα, showing the different degradation pathways and transcriptional activation of new IκBα synthesis. The newly synthesized IκBα is either degraded, binds to an NF-κB in the cytoplasm, or enters the nucleus and binds nuclear NF-κB. This feedback part of the pathway is indicated by red arrows.

biophysical origins of such a switch in degradation mechanism, and how can such a rapid signal response be initiated and subsequently repressed? The goal of this review is to illustrate that it is possible to assign reliable rates from biochemical and biophysical experiments to the apparent rate constants in the ODE model and that such an iterative process can give new insights about the behavior of the signaling module.

FOLDING DYNAMICS OF IBα

Domain Structure of IκBα. The full-length IκBα protein is composed of three major regions: an N-terminal signal response region of ~70 amino acids, where phosphorylation and ubiquitination occur, an ankyrin repeat domain (ARD) of ~220 amino acids, and a C-terminal PEST sequence that extends from residue 275 to 317 (Figure 2A) (*19*, *20*). Sequence analysis predict intrinsic disorder in both the N-terminal domain and the PEST region of IκBα as well as in a good portion of the ARD (Figure 2B) (*21*). The N-terminal domain receives the phosphorylation and ubiquitinylation signals and targets the protein to the proteasome for degradation (*9*) and has no measurable effect on binding of IκBα to NF-κB (*22*). The binding activity can be localized to the ARD and PEST regions, for which high-resolution crystal structures were obtained only when in complex with NF-κB and show that the ARD can fold as a typical elongated stack of six ARs (Figure 2C). IκBα has resisted all attempts to crystallize it in the unbound state, and its biophysical behavior is consistent with a native state that does not adopt a unique compact fold (*23*).

Theoretical Models of Folding of IκBα. ARDs are very common protein−protein interaction motifs that adopt an elongated fold in which the ankyrin repeats (ARs) stack against each other in a linear fashion by folding into two antiparallel α-helices connected by a short loop, followed by a β-hairpin that protrudes away from the helical stack (Figure 2C). This nonglobular fold is stabilized by both intra and inter-repeat interactions, and the general folding properties can be successfully modeled with simple near-neighbor interaction schemes (*24*, *25*). Theoretical folding studies using native topology-based models (*26*) (Figure 3A) and experiments (*24*, *27*−*29*) show that for natural ARDs composed of few ARs, the equilibrium folding mechanism shows a sharp transition in which once initial nucleation has occurred, the rest of the ARs fold in a highly cooperative fashion. Only the fully unfolded and fully folded species are significantly populated at equilibrium [reviewed by Barrick et al. (*30*)]. However, subtle variations in the interactions between modules may result in decoupling of the folding elements, giving rise to more complicated folding scenarios in which partially folded intermediates and multiple folding routes can be detected (*31*).

In the case of IκBα, native topology-based models using the structure of IκBα taken from the structure in complex with NF-κB predict that two separate folding events are necessary to attain complete folding, each encompassing the folding of roughly three consecutive ARs. The folding nucleates around AR2 and AR3 and propagates outward to include AR1 and AR4. Folding of AR5 and AR6 is predicted to occur in a second folding transition (Figure 3C). Thus, the ARD of IκBα behaves more like larger ARDs, which have been shown both by theory and by experiment to allow for "cracks" to occur and folding subdomains to emerge (*32*, *33*).

IκBα Deviates from the Consensus Sequence for Stable ARs. Bioinformatic analysis of the hundreds of AR sequences has resulted in several attempts to define a consensus sequence for the AR (*34*−*39*). Full-consensus ARDs have been constructed, and these exhibit much higher thermal and chemical stability as well as faster folding rates than naturally occurring ARDs similar in size (*36*−*38*, *40*−*42*). Approximately 50% of the IκBα sequence conforms to the minimum consensus and is marginally stable (Figure 4B).

Like many proteins with weakly folded parts, IκBα is prone to aggregation when isolated, even at physiological temperatures (*23*). Although this feature precludes any strict quantification of its thermal denaturation, IκBα can be reversibly denatured by chemical denaturants and its folding properties analyzed in detail (*43*). Upon denaturant challenge, the equilibrium folding behavior of the IκBα ARD (residues 67−287) shows two transitions: a minor noncooperative conversion upon subtle perturbation and a major cooperative folding event. Via introduction of Trp

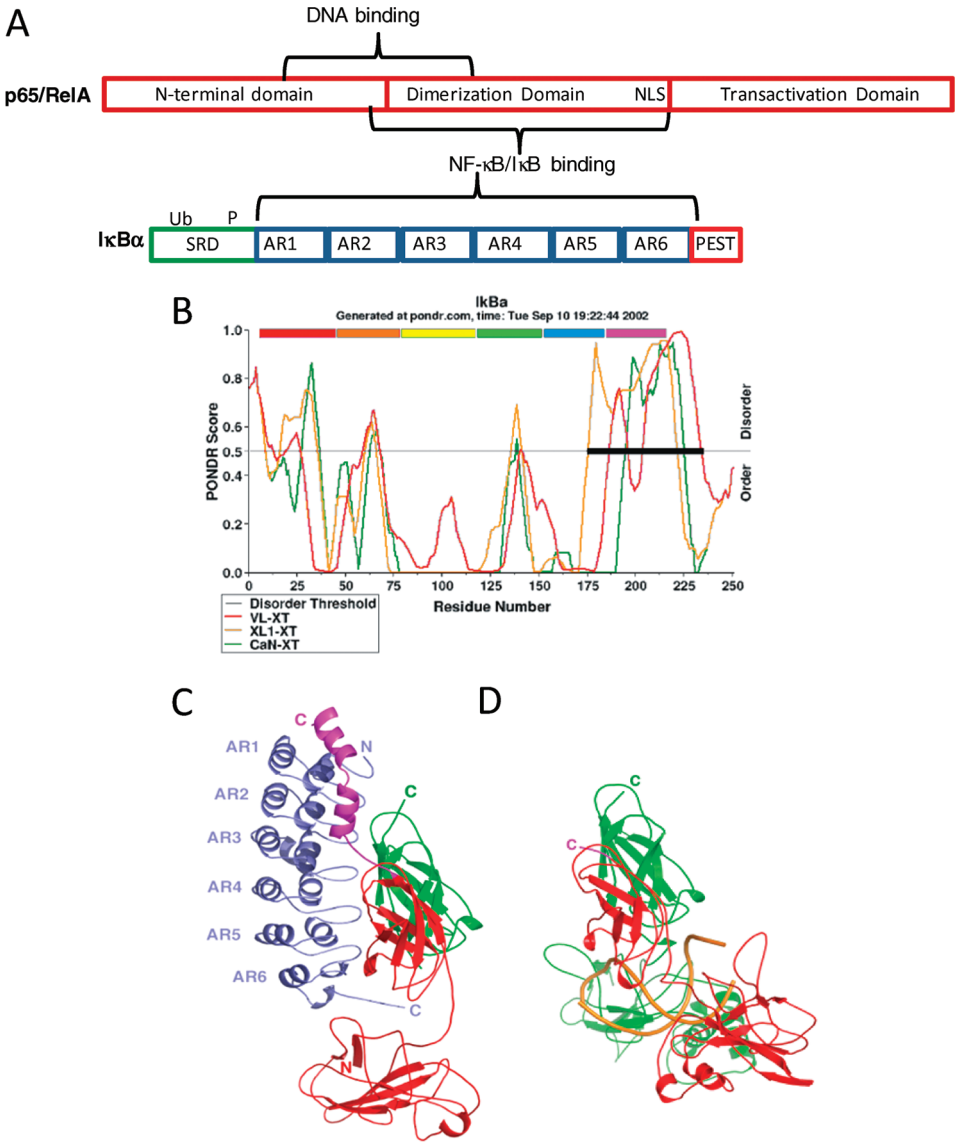

FIGURE 2: (A) Schematic diagram of NF-κB(p65), one of the most abundant NF-κB family members in the cell, and of IκBα, the key member of the inhibitor family. (B) PONDR (*21*) analysis of the intrinsic disorder in the ankyrin repeat domain of IκBα. (C) Crystal structure of IκBα (blue) bound to NF-κB (p50, green; p65, red) (*19*). (D) Crystal structure of NF-κB (p50, green; p65, red) bound to κB site DNA (gold) (*46*). This figure was prepared using *The PyMOL Molecular Graphics System* (*64*).

residues as spectroscopic probes at several positions, the non-cooperative conversion was mapped to AR5 and AR6 (*43*). The single native Trp at position 258 in AR6 does not follow a cooperative transition in the wild-type protein. However, introduction of two consensus residues (Y254L and T257A) stabilizes AR6 such that Trp258 then follows the cooperative unfolding transition of the whole ARD (Figure 4B) (*44*). On the basis of the consensus design principles, a library of mutants with varying properties of folding and stability can be engineered and quantitatively studied. If the folding properties are conserved in the cellular milieu, these can be used as a molecular toolbox to perturb elementary parameters of the signaling network.

IBα FOLDING IS COUPLED TO NF-B BINDING

Evidence of Folding upon Binding from H−D Exchange. Native state amide H−D exchange experiments followed by mass spectrometry recapitulated the theoretical results for IκBα folding transitions (Figure 3D). The β-hairpins of AR2 and AR3 were remarkably resistant to exchange, whereas AR5 and AR6 exchanged completely within the first minute in free IκBα. When bound to NF-κB, the β-hairpins of AR5 and AR6 exhibited dramatically less exchange (Figure 3D) (*45*). Interface protection could not account for the decrease in the number of exchanging amides, suggesting that IκBα undergoes a folding transition upon binding.

Structure and Energetics of Formation of the IκBα·NF-κB Complex. From the primary sequence viewpoint, NF-κB and IκBα bind in a head-to-tail fashion with the N-terminal domain of NF-κB near the C-terminal PEST sequence of IκBα (*19*, *20*). The Rel homology domain (RHD) of NF-κBs specifically binds both DNA and IκBs. Crystal structures of DNA-bound NF-κB(p50/p65) and IκBα-bound NF-κB(p50/p65) show overlapping but nonidentical binding surfaces (*19*, *20*, *46*, *47*) (Figure 2C,D). DNA contacts the loops protruding from the dimerization and N-terminal domains of the RHD and the linker between them, whereas IκBα contacts mainly the dimerization domain and the helix 3−NLS−helix 4 structure at the C-terminus of the RHD of p65 (compare panels C and D of Figure 2). How is binding energy distributed in this complex macromolecular assembly?

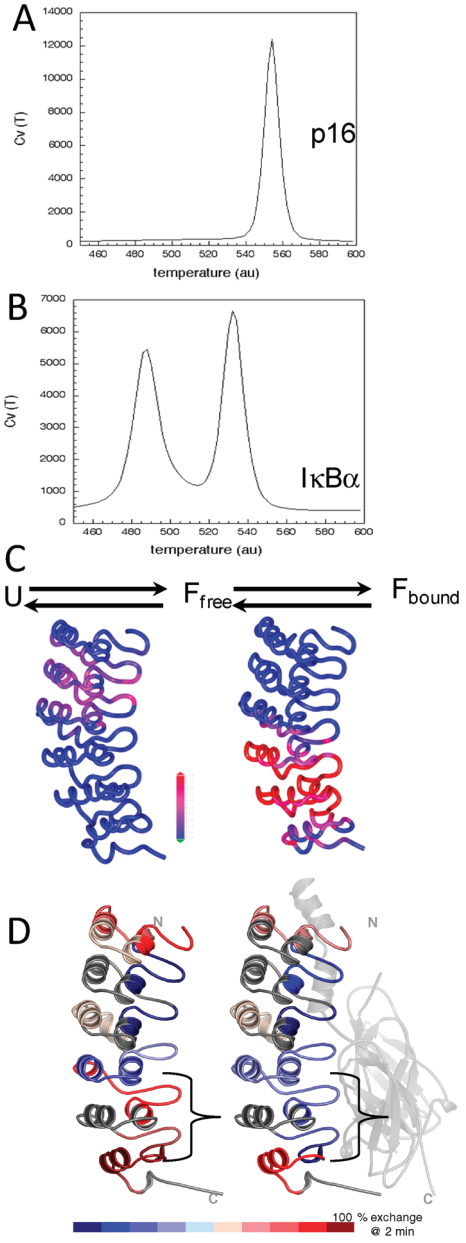

FIGURE 3: (A) Folding simulations of p16, an example ankyrin repeat protein. The folding of p16 was simulated with energetically unfrustrated models. The heat capacity as a function of temperature derived from several constant temperature runs is plotted. The peak in the plot corresponds to the folding temperature (T_f). (B) Similar analysis as in panel A but for the ARD of IκBα (residues 67−287). (C) Probability of contact formation during folding simulations of IκBα-(67−287) at the first T_f (left) and at the second T_f (right). The probability is plotted on a color scale with the most probable colored red. (D) Results from amide H−D exchange experiments with IκBα free in solution (left) and when bound to NF-κB (right). The amount of exchange was measured after exposure for 2 min to deuterated buffer followed by pepsin digestion and mass spectrometry. The extent of exchange is plotted on a color scale with the most exchanged colored red.

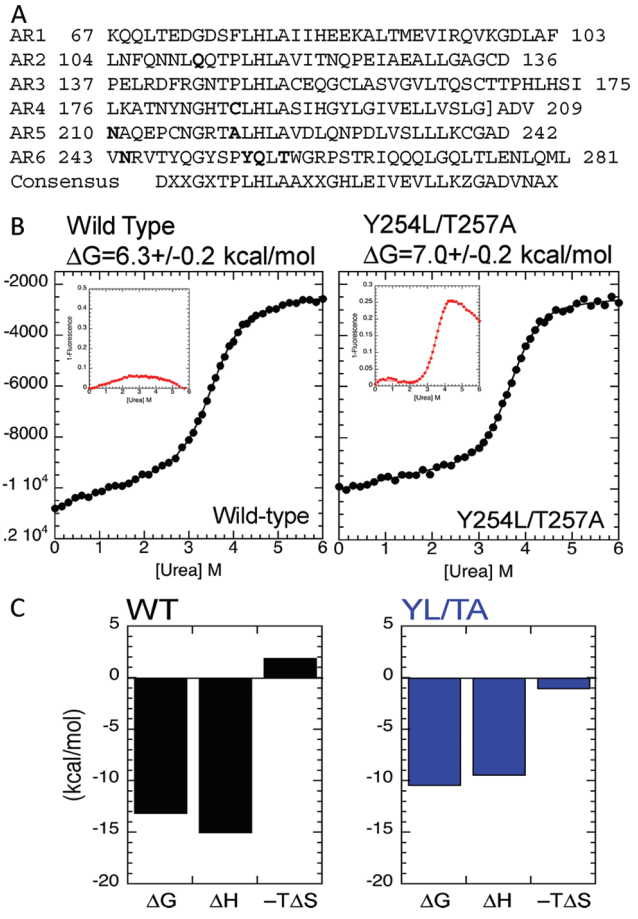

FIGURE 4: (A) Sequence of IκBα showing locations of some of the substitutions that stabilize the protein. (B) Equilibrium unfolding experiments with wild-type (left) and Y254L/T257A mutant (right) IκBα. The insets show the change in fluorescence of W258, a naturally occurring Trp in AR6. In the wild-type protein, this residue does not change fluorescence appreciably with denaturant; however, in the stabilized mutant, its fluorescence changes in a manner similar to that of the CD signal, indicating it follows the major cooperative folding transition of the protein. (C) Plots of the thermodynamic parameters of binding of wild-type (left) and Y254L/T257A mutant (right) forms of IκBα to NF-κB($p50_{248-350}/p65_{190-321}$) determined by ITC.

The protein−protein interface that forms between NF-κB and IκBα is large, having some 4000 Å^2 of buried surface area, yet mutations of interface residues had little affect on the binding free energy (Figure 4C) (*48*). Instead, all of the binding energy is attributable to interactions occurring at the two ends of the complex. At the very C-terminal end of the RHD is the nuclear localization signal (NLS polypeptide), which connects the dimerization domain to the transactivation domain in the full-length NF-κB(p65) protein (Figure 2C). The KRKR sequence, which constitutes the minimal NLS, is between two helical segments in the structure of IκBα-bound NF-κB (*19*). Deletion of the last part of this region of NF-κB, helix 4 (residues 305−321), reduces IκBα binding affinity by 7.8 kcal/mol (*8*). Theoretical studies of the binding of the NLS polypeptide (residues 291−325) of NF-κB(p65) to IκBα suggested that this segment of NF-κB folds on binding to IκBα (*53*). NMR experiments also show large chemical shift changes upon binding, consistent with the transition from mainly random coil to a helical fold (C. F. Cervantes et al., manuscript in preparation). It has been experimentally observed that this segment binds to IκBα with a K_D of 1 μM, and with a large $\Delta C_{p,obs}$ for binding of IκBα to this NLS segment (-1.30 ± 0.03 kcal mol^{-1} K^{-1}). Calculations of burial of polar and nonpolar surface area derived from the crystal structures could not account for this large effect (*49*−*51*). Thus, merely docking the individual static structures cannot account for the thermodynamic signatures of the binding interaction, and larger structural rearrangements must be implicated, which is often observed for protein−DNA interactions (*52*). Thus, the "head" of IκBα (ARs 1−3) appears to be folded on the basis of H−D

exchange experiments, and the "tail" of NF-κB (the NLS polypeptide) folds upon binding to it.

At the other end of the IκBα ARD, deletion of the PEST sequence (residues 276−287) reduces the level of NF-κB binding by some 5 kcal/mol (*54*). Taken together, the binding affinity losses due to deletion at the ends of the interface are more than enough to account for the entire binding energy of complex formation. Interestingly, the PEST region does not become completely ordered upon binding to NF-κB according to high-resolution NMR spectroscopy data (*55*). The native state of the NF-κB·IκBα complex thus retains regions with highly dynamic character. Given that AR5 and AR6 at one end of the interface and the NLS at the other end of the interface both fold on binding, the folding energy landscape of both proteins must be taken into account in analyzing the binding event.

Alteration of Binding Thermodynamics by Stabilizing Mutations. It is important to emphasize that AR5 and AR6 of IκBα in the free state are not random coil or completely unfolded. Indeed, even though the amides in these two repeats completely exchange in <1 min, no new secondary structure forms when IκBα binds to NF-κB (*23*). Thus, the AR5−AR6 region must be partially folded, perhaps molten globular in the free state. Further evidence of the partially folded state of the AR5−AR6 region comes from studies on the thermodynamics of binding of wild-type and mutant forms of IκBα.

The aforementioned Y254L/T257A mutant exhibited a markedly changed equilibrium folding profile compared to that of wild-type IκBα (Figure 4B). Indeed, one can conclude that AR5 and AR6 now form part of the cooperatively folding ARD. Binding thermodynamics of this locally stabilized mutant IκBα compared to the wild type allowed us to speculate about how the very tight binding affinity of IκBα for NF-κB is achieved. The unfavorable entropy change upon binding of wild-type IκBα is smaller than would be expected if the residues in AR5 and AR6 (some 80 amino acids) of IκBα were undergoing a transition from completely unfolded to completely folded (Figure 4C). To a first approximation, if folding is coupled to binding, stabilizing a weakly folded protein should strengthen binding as the unfavorable folding entropy should be decreased. The stabilized mutant did, indeed, have a less unfavorable entropy change upon binding, but the effect was only ∼2 kcal/mol. Surprisingly, the binding affinity of the stabilized mutant IκBα for NF-κB was weakened some 30-fold, due to a much less favorable enthalpy change upon binding (Figure 4C). Our interpretation of this result is that if the free IκBα is molten globular, it has already paid most of the entropy cost of folding (and gained most of the favorable entropy from the hydrophobic effect) but has not completely attained the favorable enthalpy of the folded state. An alternative interpretation is that the stabilized mutant cannot structurally adapt to access the conformation required for optimal binding of NF-κB.

Possible Entropy Compensation upon Binding. Even with the model just described, it is still surprising that the entropy cost upon binding is so small considering one-third of IκBα is weakly folded when free in solution (*45*). A possible explanation is that some other part of the ARD becomes more dynamic upon binding and compensates for the entropy cost of folding AR5 and AR6. NMR backbone dynamics experiments revealed that some entropy compensation of this type may be occurring. Surprisingly, although AR2 and AR3 are the most well-folded, a large number of the resonances in AR3 that are observed in the NMR spectrum of free IκBα(67−206) are actually not observed in the NMR spectrum of IκBα(67−287) in complex with NF-κB (*56*). When amide cross-peaks are not visible in the NMR spectrum, this is usually evidence of intermediate exchange on the NMR time scale, a phenomenon indicative of micro- to millisecond dynamics. Given the subnanomolar binding affinity of the NF-κB·IκBα complex, these dynamics must be regarded as an increase in backbone dynamics within the complex and not a result of an association−dissociation process. Such an increase in dynamics suggests a redistribution of disorder so that the loss of entropy in AR5 and AR6 may be offset by an increase in the amount of AR3. Backbone relaxation measurements and analysis of long-time scale dynamics from residual dipolar coupling experiments on the free IκBα(67−206) revealed that although AR3 is in the core of the folded part of IκBα, parts of this AR are more dynamic than the other ARs even in the free state (*57*).

IBα FOLDING DETERMINES ITS INTRACELLULAR HALF-LIFE

Distinct Degradation Pathways for IκBα. It is generally believed (although not thoroughly tested) that, in the absence of active mechanisms of degradation, the more thermodynamically stable a protein, the longer its in vivo half-life. Consistent with this notion, free IκBα, which is marginally stable (*23*), has a very short intracellular half-life of <10 min (*17*, *58*). This rapid degradation rate depends in part on the presence of the C-terminal PEST sequence (*18*, *59*, *60*). The degradation of the free protein appears to be independent of ubiquitinylation, since all of the Lys residues in IκBα can be mutated without changing the degradation rate of the free protein (*18*). In addition, although free IκBα can be phosphorylated and ubiquitinylated, its degradation rate is not different in IKK−/− cells, indicating that ubiquitin-independent degradation is the primary route for free IκBα (*17*). The Y254L/T257A mutant IκBα is degraded more slowly than wild-type IκBα both in vitro by the 20S proteasome and in vivo, suggesting that in addition to the PEST sequence, the weakly folded AR6 of IκBα is important for rapid ubiquitin-independent degradation (Figure 5B,C) (*44*).

When IκBα is bound to NF-κB, they form a very stable complex that requires ubiquitinylation for degradation by the Ub-dependent degradation pathway that uses the ATPases of the 26S subunit to unfold and subsequently degrade the protein. Our studies showing that the binding affinity for the NF-κB-bound IκBα is concentrated in two regions at the ends of the interface suggest a mechanism for proteasome degradation of the NF-κB-bound IκBα. If proteasome digestion starts near the N-terminal ubiquitinylated residues of IκBα and proceeds to AR1, this would disrupt the interaction between AR1 and the NLS polypeptide [residues 305−325 of NF-κB(p65)]. We know from deletion studies that the interaction between the NLS polypeptide and AR1 is worth some 8000-fold in binding affinity, and disruption of this interaction causes the NF-κB to rapidly dissociate (*8*).

Intracellular Half-Life of IκBα Is a Critical Parameter for Signaling Control. An ordinary differential equation (ODE) model of the NF-κB signaling system has been constructed that recapitulates the interesting oscillatory behavior of the NF-κB transcription activity (Figure 5A) (*1*). Such ODE models are informative because one can test them for sensitivity of each of the parameters to computationally dissect the system's behavior. In the case of NF-κB signaling, one of the most sensitive parameters for control of the constitutive transcriptional activity is the intracellular half-life of IκBα (*17*). Recent reparameterization of this model shows that when the binding

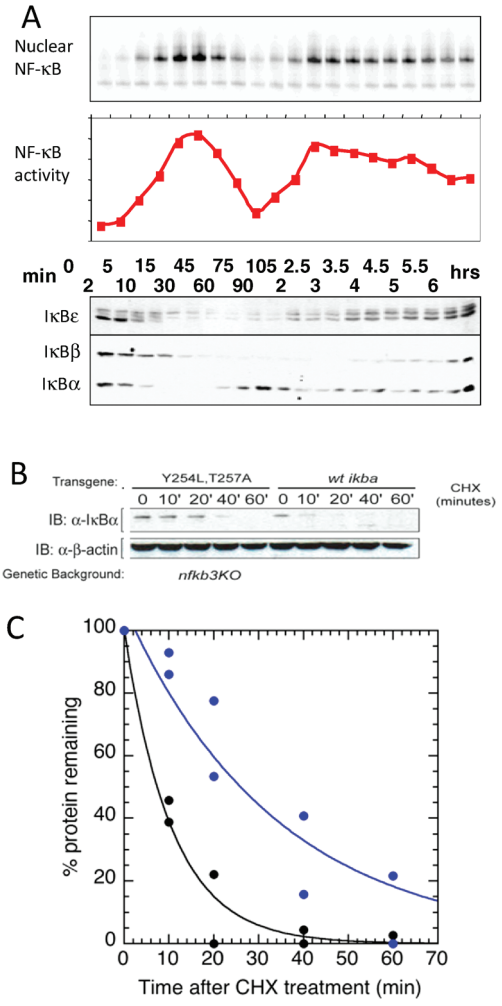

FIGURE 5: (A) NF-κB transcription activity was measured as a function of time after stimulation with tumor necrosis factor. Proteins were also measured by quantitative Western blotting: (top) NF-κB(p65) and (bottom) IκB isoforms. (B) Quantitative Western blot showing the levels of IκBα(Y254L/T257A) and the wild type after cyclohexamide treatment in NF-κB −/− cells.

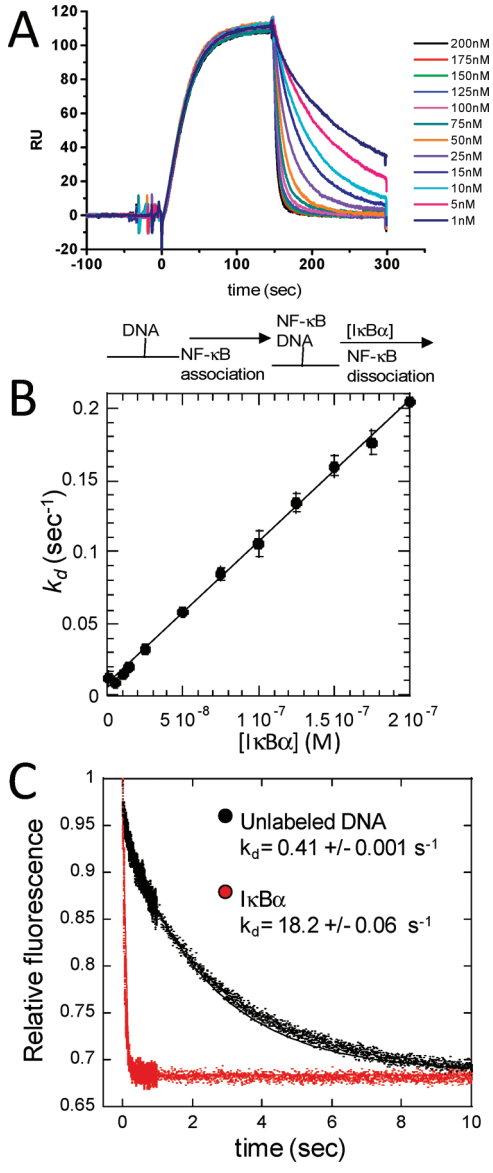

FIGURE 6: (A) Real-time binding and dissociation experiment monitored by SPR. Biotinylated κB-site DNA was bound to the streptavidin chip (t = 0). NF-κB(p50$_{(19-363)}$/p65$_{(1-325)}$) was allowed to associate with the DNA until a pseudoflowing equilibrium was reached (t = 100 s). Varying concentrations of IκBα were then injected through the second sample loop (coinject experiment), and the dissociation rate constant (k_d) was measured. A schematic of the binding events is shown below the graph. (B) Plot of the k_d determined from experiments like that shown in panel A as a function of IκBα concentration. The error bars represent four independent experiments. The slope of the line is the pseudo-second-order rate constant for IκBα-mediated dissociation, and its value of 10^6 M^{-1} s^{-1} indicates that IκBα-mediated active dissociation is a very efficient process. (C) Dissociation was also monitored by stopped-flow fluorimetry using a pyrene-labeled DNA hairpin. Stopped-flow fluorescence experiment in which pyrene-labeled hairpin DNA (0.25 μM) in a complex with NF-κB(p50$_{(19-363)}$/p65$_{(1-325)}$) (0.5 μM) in syringe 1 was rapidly mixed with a 50-fold excess (relative to NF-κB) of either unlabeled hairpin DNA (black curve; k_d = 0.41 s^{-1}) or IκBα (red curve; k_d = 18.2 s^{-1}).

rates and affinities measured in vitro by SPR are used as fixed parameters, the model recapitulates the rates and amplitudes of the NF-κB response. SPR experiments revealed the extremely slow dissociation rate of the IκBα·NF-κB complex, consistent with the long intracellular half-life of the complex, which is completely stable in the absence of IκB kinase (IKK) phosphorylation and subsequent ubiquitinylation (>12 h). Thus, IκBα "foldedness", controlled by binding to NF-κB, allows it to switch between degradation mechanisms (*18*).

RAPID TRANSCRIPTION REPRESSION REQUIRES PARTIALLY FOLDED IBα

A key feature of the NF-κB negative feedback is the rapidity with which the transcriptional activation is subsequently repressed (Figure 5A) (*1*). The rapid postinduction repression is partly explained by the fact that the gene for IκBα is strongly induced by NF-κB, so activation of NF-κB immediately produces newly synthesized IκBα. However, the new IκBα must still escape proteasome degradation, enter the nucleus, and compete for binding to NF-κB with the very large number of κB sites in the DNA. We recently discovered an intriguing kinetic phenomenon in which IκBα is able to markedly increase the rate of dissociation of NF-κB from the DNA (*61*). The phenomenon was initially discovered by passing nanomolar concentrations of IκBα over the NF-κB·DNA complex in a co-injection step in an SPR experiment (Figure 6A). IκBα is remarkably efficient at increasing the rate of dissociation (k_d) of NF-κB from the DNA; the apparent second-order rate constant for the IκBα-mediated

dissociation is $10^6\ M^{-1}\ s^{-1}$ (Figure 6B). Similar experiments were also performed using stopped-flow fluorescence; the same phenomenon was observed under solution conditions (Figure 6C). Several mutant forms of IκBα were also tested for their ability to mediate dissociation of NF-κB from the DNA. The mutations had a variety of effects on NF-κB binding, from none to a decrease of some 100-fold. However, all of the thermodynamically stabilized mutants, even the ones that bound with the same affinity, were less able to mediate dissociation of NF-κB from the DNA (*61*). Thus, an important function of the "weakly folded" part of IκBα may be to facilitate dissociation of NF-κB from the DNA to rapidly repress postinduction transcriptional activation.

CONCLUDING REMARKS AND PERSPECTIVES

Although the NF-κB signaling module comprises only a small portion of the entire cellular signaling network, it has intriguing complexities. The importance of biochemical and biophysical experiments that seek a quantitative understanding of such signaling modules cannot be underestimated. If we are to build up a quantitative and robust description of cellular signaling, the interplay between rigorous biophysical measurements and cell biological experiments as well as comprehensive mathematical models that reveal the emerging properties of the system will all be essential (*62*, *63*). Protein−protein interactions play a fundamental role in intracellular signaling, but simple models that assume equilibrium binding under cellular conditions will not suffice. Signaling networks depend upon protein−protein interactions that can be under kinetic as well as thermodynamic control. We have shown that the structural and dynamic features of IκBα, in particular, its foldedness, are exploited to provide kinetic control of dynamic regulatory processes, including its degradation through Ub-dependent and -independent pathways and competition with DNA for NF-κB.

When quantitative in vitro experiments can be racapitulated in cellular models, emergent properties of the cellular control can be discovered. For example, the observation of a kinetic control mechanism in the NF-κB signaling module raises the possibility that when the model is more complete, the number of newly synthesized IκBα molecules that enter the nucleus during postinduction repression may be very low, and single molecules may be able to remove NF-κB from transcription sites requiring inclusion of stochastic processes in addition to the equilibrium flux equations to accurately model the entire system. The iteration between biophysical experiments and measurement of cellular properties will be critical for such a further model refinement. The converse is also true in the sense that when a protein is involved in a highly regulated cellular system, it is more likely that its interactions will be tuned to respond rapidly to changes in the regulatory state and will most likely not display simple kinetics or thermodynamics of binding.

ACKNOWLEDGMENT

We thank Gourisankar Ghosh, Peter G. Wolynes, H. Jane Dyson, and Alexander Hoffmann, who all contributed data and helpful discussion.

REFERENCES

1. Hoffmann, A., Levchenko, A., Scott, M. L., and Baltimore, D. (2002) The IκB-NF-κB signaling module: Temporal control and selective gene activation. *Science 298*, 1241–1245.
2. Ghosh, S., May, M. J., and Kopp, E. B. (1998) NF-κB and Rel proteins: Evolutionarily conserved mediators of immune responses. *Annu. Rev. Immunol. 16*, 225–260.
3. Kumar, A., Takada, Y., Boriek, A. M., and Aggarwal, B. B. (2004) Nuclear factor-κB: Its role in health and disease. *J. Mol. Med. 82*, 434–448.
4. Hoffmann, A., and Baltimore, D. (2006) Circuitry of nuclear factor κB signaling. *Immunol. Rev. 210*, 171–186.
5. Verma, I. M., Stevenson, J. K., Schwarz, E. M., Van Antwerp, D., and Miyamoto, S. (1995) Rel/NF-κ B/I κB family: Intimate tales of association and dissociation. *Genes Dev. 9*, 2723–2735.
6. Basak, S., Kim, H., Kearns, J. D., Tergaonkar, V., O'Dea, E., Werner, S. L., Benedict, C. A., Ware, C. F., Ghosh, G., Verma, I. M., and Hoffmann, A. (2007) A fourth IκB protein within the NF-κB signaling module. *Cell 128*, 369–381.
7. Baeuerle, P. A. (1998) IκB-NF-κB structures: At the interface of inflammation control. *Cell 95*, 729–731.
8. Bergqvist, S., Croy, C. H., Kjaergaard, M., Huxford, T., Ghosh, G., and Komives, E. A. (2006) Thermodynamics reveal that helix four in the NLS of NF-κB p65 anchors IκBα, forming a very stable complex. *J. Mol. Biol. 360*, 421–434.
9. Traenckner, E. B., and Baeuerle, P. A. (1995) Appearance of apparently ubiquitin-conjugated IκB-α during its phosphorylation-induced degradation in intact cells. *J. Cell Sci. Suppl. 19*, 79–84.
10. Pahl, H. L. (1999) Activators and target genes of Rel/NF-κB transcription factors. *Oncogene 18*, 6853–6866.
11. Hoffmann, A., Leung, T. H., and Baltimore, D. (2003) Genetic analysis of NF-κB/Rel transcription factors defines functional specificities. *EMBO J. 22*, 5530–5539.
12. Werner, S. L., Barken, D., and Hoffmann, A. (2005) Stimulus specificity of gene expression programs determined by temporal control of IKK activity. *Science 309*, 1857–1861.
13. Brown, K., Park, S., Kanno, T., Franzoso, G., and Siebenlist, U. (1993) Mutual regulation of the transcriptional activator NF-κB and its inhibitor, IκB-α. *Proc. Natl. Acad. Sci. U.S.A. 90*, 2532–2536.
14. Scott, M. L., Fujita, T., Liou, H. C., Nolan, G. P., and Baltimore, D. (1993) The p65 subunit of NF-κB regulates IκB by two distinct mechanisms. *Genes Dev. 7*, 1266–1276.
15. Sun, S. C., Ganchi, P. A., Ballard, D. W., and Greene, W. C. (1993) NF-κB controls expression of inhibitor IκBα: Evidence for an inducible autoregulatory pathway. *Science 259*, 1912–1915.
16. Arenzana-Seisdedos, F., Turpin, P., Rodriguez, M., Thomas, D., Hay, R. T., Virelizier, J.-L., and Dargemont, C. (1997) Nuclear localization of IκBα promotes active transport of NF-κB from the nucleus to the cytoplasm. *J. Cell Sci. 110*, 369–378.
17. O'Dea, E. L., Barken, D., Peralta, R. Q., Tran, K. T., Werner, S. L., Kearns, J. D., Levchenko, A., and Hoffmann, A. (2007) A homeostatic model of IκB metabolism to control constitutive NF-κB activity. *Mol. Syst. Biol. 3*, 111.
18. Mathes, E., O'Dea, E. L., Hoffmann, A., and Ghosh, G. (2008) NF-κB dictates the degradation pathway of IκBα. *EMBO J. 27*, 1357–1367.
19. Jacobs, M. D., and Harrison, S. C. (1998) Structure of an IκBα/NF-κB complex. *Cell 95*, 749–758.
20. Huxford, T., Huang, D. B., Malek, S., and Ghosh, G. (1998) The crystal structure of the IκBα/NF-κB complex reveals mechanisms of NF-κB inactivation. *Cell 95*, 759–770.
21. Garner, E., Romero, P., Dunker, A. K., Brown, C., and Obradovic, Z. (1999) Predicting Binding Regions within Disordered Proteins. *Genome Inf. 10*, 41–50.
22. Huxford, T., Malek, S., and Ghosh, G. (1999) Structure and mechanism in NF-κB/IκB signaling. *Cold Spring Harbor Symp. Quant. Biol. 64*, 533–540.
23. Croy, C. H., Bergqvist, S., Huxford, T., Ghosh, G., and Komives, E. A. (2004) Biophysical characterization of the free IκBα ankyrin repeat domain in solution. *Protein Sci. 13*, 1767–1777.
24. Mello, C. C., and Barrick, D. (2004) An experimentally determined protein folding energy landscape. *Proc. Natl. Acad. Sci. U.S.A. 101*, 14102–14107.
25. Ferreiro, D. U., Walczak, A. M., Komives, E. A., and Wolynes, P. G. (2008) The energy landscapes of repeat-containing proteins: Topology, cooperativity, and the folding funnels of one-dimensional architectures. *PLoS Comput. Biol. 16*, e1000070.
26. Ferreiro, D. U., Cho, S. S., Komives, E. A., and Wolynes, P. G. (2005) The energy landscape of modular repeat proteins: Topology determines folding mechanism in the ankyrin family. *J. Mol. Biol. 354*, 679–692.
27. Tang, K. S., Guralnick, B. J., Wang, W. K., Fersht, A. R., and Itzhaki, L. S. (1999) Stability and folding of the tumour suppressor protein p16. *J. Mol. Biol. 285*, 1869–1886.

28. Zweifel, M. E., and Barrick, D. (2001) Studies of the ankyrin repeats of the *Drosophila melanogaster* Notch receptor. 2. Solution stability and cooperativity of unfolding. *Biochemistry 40*, 14357–14367.
29. Zeeb, M., Rosner, H., Zeslawski, W., Canet, D., Holak, T. A., and Balbach, J. (2002) Protein Folding and Stability of Human CDK Inhibitor p19INK4d. *J. Mol. Biol. 315*, 447–457.
30. Barrick, D., Ferreiro, D. U., and Komives, E. A. (2008) Folding landscapes of ankyrin repeat proteins: Experiments meet theory. *Curr. Opin. Struct. Biol. 18*, 27–34.
31. Lowe, A. R., and Itzhaki, L. S. (2007) Rational redesign of the folding pathway of a modular protein. *Proc. Natl. Acad. Sci. U.S.A. 104*, 2679–2684.
32. Löw, C., Weininger, U., Zeeb, M., Zhang, W., Laue, E. D., Schmid, F. X., and Balbach, J. (2007) Folding Mechanism of an Ankyrin Repeat Protein: Scaffold and Active Site Formation of Human CDK Inhibitor p19INK4d. *J. Mol. Biol. 373*, 219–231.
33. Werbeck, N. D., and Itzhaki, L. S. (2007) Probing a moving target with a plastic unfolding intermediate of an ankyrin repeat protein. *Proc. Natl. Acad. Sci. U.S.A. 104*, 7863–7868.
34. Michaely, P., and Bennett, V. (1992) The ANK repeat: A ubiquitous motif involved in macromolecular recognition. *Trends Cell Biol. 2*, 127–129.
35. Sedgwick, S. G., and Smerdon, S. J. (1999) The ankyrin repeat: A diversity of interactions on a common structural framework. *Trends Biochem. Sci. 24*, 311–316.
36. Mosavi, L. K., Minor, D. L., Jr., and Peng, Z. Y. (2002) Consensus-derived structural determinants of the ankyrin repeat motif. *Proc. Natl. Acad. Sci. U.S.A. 99*, 16029–16034.
37. Binz, H. K., Stumpp, M. T., Forrer, P., Amstutz, P., and Pluckthun, A. (2003) Designing repeat proteins: Well-expressed, soluble and stable proteins from combinatorial libraries of consensus ankyrin repeat proteins. *J. Mol. Biol. 332*, 489–503.
38. Kohl, A., Binz, H. K., Forrer, P., Stumpp, M. T., Pluckthun, A., and Grutter, M. G. (2003) Designed to be stable: Crystal structure of a consensus ankyrin repeat protein. *Proc. Natl. Acad. Sci. U.S.A. 100*, 1700–1705.
39. Tripp, K. W., and Barrick, D. (2007) Enhancing the stability and folding rate of a repeat protein through the addition of consensus repeats. *J. Mol. Biol. 365*, 1187–1200.
40. Devi, V. S., Binz, H. K., Stumpp, M. T., Pluckthun, A., Bosshard, H. R., and Jelesarov, I. (2004) Folding of a designed simple ankyrin repeat protein. *Protein Sci. 13*, 2864–2870.
41. Interlandi, G., Wetzel, S. K., Settanni, G., Pluckthun, A., and Caflisch, A. (2008) Characterization and further stabilization of designed ankyrin repeat proteins by combining molecular dynamics simulations and experiments. *J. Mol. Biol. 375*, 837–854.
42. Wetzel, S. K., Settanni, G., Kenig, M., Binz, H. K., and Pluckthun, A. (2008) Folding and unfolding mechanism of highly stable full-consensus ankyrin repeat proteins. *J. Mol. Biol. 376*, 241–257.
43. Ferreiro, D. U., Cervantes, C. F., Truhlar, S. M., Cho, S. S., Wolynes, P. G., and Komives, E. A. (2007) Stabilizing IκBα by "consensus" design. *J. Mol. Biol. 365*, 1201–1216.
44. Truhlar, S. M. E., Mathes, E., Cervantes, C. F., Ghosh, G., and Komives, E. A. (2008) Pre-folding IκBα alters control of NF-κB signaling. *J. Mol. Biol. 380*, 67–82.
45. Truhlar, S. M., Torpey, J. W., and Komives, E. A. (2006) Regions of IκBα that are critical for its inhibition of NF-κB·DNA interaction fold upon binding to NF-κB. *Proc. Natl. Acad. Sci. U.S.A. 103*, 18951–18956.
46. Chen, F. E., Huang, D. B., Chen, Y. Q., and Ghosh, G. (1998) Crystal structure of p50/p65 heterodimer of transcription factor NF-κB bound to DNA. *Nature 391*, 410–413.
47. Müller, C. W., Rey, F. A., Sodeoka, M., Verdine, G. L., and Harrison, S. C. (1995) Structure of the NF-κB p50 homodimer bound to DNA. *Nature 373*, 311–317.
48. Huxford, T., Mishler, D., Phelps, C. B., Huang, D. B., Sengchanthalangsy, L. L., Reeves, R., Hughes, C. A., Komives, E. A., and Ghosh, G. (2002) Solvent exposed non-contacting amino acids play a critical role in NF-κB/IκBα complex formation. *J. Mol. Biol. 324*, 587–597.
49. Ha, J. H., Spolar, R. S., and Record, M. T. (1989) Role of the Hydrophobic Effect in Stability of Site-Specific Protein-DNA Complexes. *J. Mol. Biol. 209*, 801–816.
50. Livingstone, J. R., Spolar, R. S., and Record, M. T. (1991) Contribution to the Thermodynamics of Protein Folding from the Reduction in Water-Accessible Nonpolar Surface Area. *Biochemistry 30*, 4237–4244.
51. Spolar, R. S., Livingstone, J. R., and Record, M. T. (1992) Use of Liquid-Hydrocarbon and Amide Transfer Data to Estimate Contributions to Thermodynamic Functions of Protein Folding from the Removal of Nonpolar and Polar Surface from Water. *Biochemistry 31*, 3947–3955.
52. Spolar, R. S., and Record, J. M. T. (1994) Coupling of Local Folding to Site-Specific Binding of Proteins to DNA. *Science 263*, 777–784.
53. Latzer, J., Papoian, G. A., Prentiss, M. C., Komives, E. A., and Wolynes, P. G. (2007) Induced fit, folding, and recognition of the NF-κB-nuclear localization signals by IκBα and IκBβ. *J. Mol. Biol. 367*, 262–274.
54. Bergqvist, S., Ghosh, G., and Komives, E. A. (2008) The IκBα/NF-κB complex has two hot-spots, one at either end of the interface. *Protein Sci. 17*, 2051–2058.
55. Sue, S. C., and Dyson, H. J. (2009) Interaction of the IκBα C-terminal PEST sequence with NF-κB: Insights into the inhibition of NF-κB DNA binding by IκBα. *J. Mol. Biol. 388*, 824–838.
56. Sue, S. C., Cervantes, C., Komives, E. A., and Dyson, H. J. (2008) Transfer of Flexibility between Ankyrin Repeats in IκBα upon Formation of the NF-κB Complex. *J. Mol. Biol. 380*, 917–931.
57. Cervantes, C. F., Markwick, P. R. L., Sue, S. C., McCammon, J. A., Dyson, H. J., and Komives, E. A. (2009) Functional dynamics of the folded ankyrin repeats of IκBα revealed by nuclear magnetic resonance. *Biochemistry 48*, 8023–8031.
58. Rogers, S., Wells, R., and Rechsteiner, M. (1986) Amino acid sequences common to rapidly degraded proteins: The PEST hypothesis. *Science 234*, 364–368.
59. Rice, N. R., and Ernst, M. K. (1993) In vivo control of NF-κB activation by IκBα. *EMBO J. 12*, 4685–4695.
60. Pando, M. P., and Verma, I. M. (2000) Signal-dependent and -independent degradation of free and NF-κB bound IκBα. *J. Biol. Chem. 275*, 21278–21286.
61. Bergqvist, S., Alverdi, V., Mengel, B., Hoffmann, A., Ghosh, G., and Komives, E. A. (2009) Kinetic enhancement of NF-κB·DNA dissociation by IκBα. *Proc. Natl. Acad. Sci. U.S.A. 106*, 19328–19333.
62. Wu, J. Q., McCormick, C. D., and Pollard, T. D. (2008) Counting proteins in living cells by quantitative fluorescence microscopy with internal standards. *Methods Cell Biol. 89*, 253–273.
63. Pollard, T. D., and Berro, J. (2009) Mathematical models and simulations of cellular processes based on actin filaments. *J. Biol. Chem. 284*, 5433–5437.
64. DeLano, W. L. (2002) The PyMOL Molecular Graphics System, DeLano Scientific, San Carlos, CA.